Int. J. Electrochem. Sci., 7 **(2012)** 9303 - 9324

International Journal of
ELECTROCHEMICAL
SCIENCE
www.electrochemsci.org

Exudate Gum from *Acacia Trees* as Green Corrosion Inhibitor for Mild Steel in Acidic Media

M. A. Abu-Dalo[1], *A. A.Othman*[2], *N. A.F. Al-Rawashdeh*[1,3,*]

[1] Department of Applied Chemical Sciences, Jordan University of Science and Technology, Irbid, Jordan.
[2] Department of Chemistry, College of Science and General Studies, Alfaisal University, Riyadh, Saudi Arabia.
[3] Department of Chemistry, College of Science, United Arab Emirates University, Al Ain, Abu Dhabi, UAE.
[*]E-mail: nathir@uaeu.ac.ae

Received: 5 August 2012 / *Accepted:* 4 September 2012 / *Published:* 1 October 2012

The inhibition effect of exudate gum from *Acacia trees* (*Gum Acacia*, GA) on the corrosion of mild steel in acidic media was studied by weight loss, hydrogen evolution, and electrochemical polarization methods; also, surface morphology was analyzed by Fourier transform infrared spectroscopy (FTIR), scanning electron microscopy (SEM), and X-ray photoelectron spectroscopy (XPS) techniques. The results of weight loss, hydrogen evolution, and electrochemical polarization methods indicated that inhibitor efficiency (I%) increased with increasing inhibitor concentration. The inhibitor efficiency (I%) in hydrochloric acid is much more than those in sulfuric acid due to the synergistic effect. The percentage inhibition efficiency (I%) of steel corrosion with GA is highly increased in the presence of an external magnetic field. Results of weight loss method are highly consistent with those obtained by hydrogen evolution method, and both indicate that inhibitor efficiency increases with increasing inhibitor concentration and the presence of external magnetic field. Electrochemical polarization studies showed that *Gum Acacia* acts as mixed type inhibitors. The results reveal that *Gum Acacia* provided a very good protection to mild steel against corrosion in acidic media. FTIR, SEM and XPS confirmed the existence of an absorbed protective film on the mild steel surface.

Keywords: mild steel; *Acacia* trees; weight loss; hydrogen evolution; polarization; acid inhibition

1. INTRODUCTION

Mild steel is the most common form of steel because of its relatively low cost and material properties that are acceptable for many applications particularly in food, petroleum, chemical and

electrochemical industries, and power production. The major problem of mild steel in many industries is its dissolution in acidic medium where acids are widely used for applications such as acid pickling, acid cleaning, acid descaling, and oil well acidizing.

In order to protect mild steel from corrosion, corrosion inhibitors are widely used in industry to control metal dissolution and reduce the corrosion rate in contact with aggressive acid solution. Most acid inhibitors are organic compounds containing nitrogen, sulphur and/or oxygen in their molecule [1-4]. The inhibition action is due to the formation of protection film on to the metal surface blocking the metal from the corrosive agents present in solution. A great number of scientific studies have been dedicated to the corrosion of mild steel and the use of organic compounds as corrosion inhibitors in acidic media [4, 5-6]. Because most of these synthetic organic inhibitors are expensive and toxic to the environment, investigation and evaluation of naturally occurring substances (organic inhibitors) has continued to receive attention due to the presence of hetero atoms like nitrogen, sulfur and oxygen in their structure. Many researchers examined various naturally occurring substances as corrosion inhibitors for different metals in various environments, and reported their metals corrosion inhibitive effectiveness in aggressive solutions [7-13]. Recently, Sangeetha et al. [14] review in detail the green corrosion inhibitors that have been used.

Gum Acacia (GA) is of particular interest because of their safe use, high solubility in water and high molecular size. It is a multifraction material consisting mainly of highly branched polysaccharides (Figure 1) (typically 42% galactosyl, 27% arabinosyl, 15% rhamnosyl, 14.5% glucuronosyl, and 1.5% 4-O-methyl-glucuronosyl) and a protein-polysaccharide complex as a minor component [15]. GA consists of mainly three fractions [16]: (1) The major one is a highly branched polysaccharide (MW = 3×10^5) consisting of β-(1→3) galactose backbone with linked branches of arabinose and rhamnose, which terminate in glucuronic acid (found in nature as magnesium, potassium, and calcium salt). (2) A smaller fraction (~10 wt % of the total) is a higher molecular weight (~1×10^6 g/mol) arabinogalactan–protein complex (GAGP –GA glycoprotein) in which arabinogalactan chains are covalently linked to a protein chain through serine and hydroxyproline groups. The attached arabinogalactan in the complex contains ~13% (by mole) glucoronic acid. (3) The smallest fraction (~1% of the total) having the highest protein content (~50 wt %) is a glycoprotein which differs in its amino acids composition from that of the GAGP complex [16]. It is obtained from the Acacia tree which grows in a region that stretches from Senegal to Sudan in Africa [17]. However, its composition can vary with its source, the age of the trees, soil environment and climatic conditions [17-20]. Idris et al. [18] reported GA to comprise 39–42% galactose, 24–27% arabinose, 12–16% rhamnose, 15–16% glucuronic acid, 1.5–2.6% protein, 0.22–0.39% nitrogen, and 12.5–16.0% moisture. GA has wide industrial uses as a stabilizer, thickening agent and emulsifier, mainly in the food industry but also in the textile, pottery, lithography, cosmetics and pharmaceutical industries [18]. Investigations on exudates gums from *Pachylobus eduli, Dacroydes edulis* and *Raphia hookeri* for aluminum and mild steel in hydrochloric and sulfuric acids in the presence and absence of halide ions reported that the inhibition efficiency depends on GA concentration, temperature and the presence of halide ions [21,22]. The reported observations were attributed to the presence of arabinogalactan, oligosaccharides, polysaccharides and glucoproteins. In addition, *Gum Acacia* was found to be a good inhibitor for both mild steel and aluminum in both acidic and alkaline media and being a better inhibitor for aluminum than for mild

steel [23,24]. However, data on the active materials of *Gum Acacia* in the adsorbed layer is unavailable, and the small amount of literature available on this subject is tenuous.

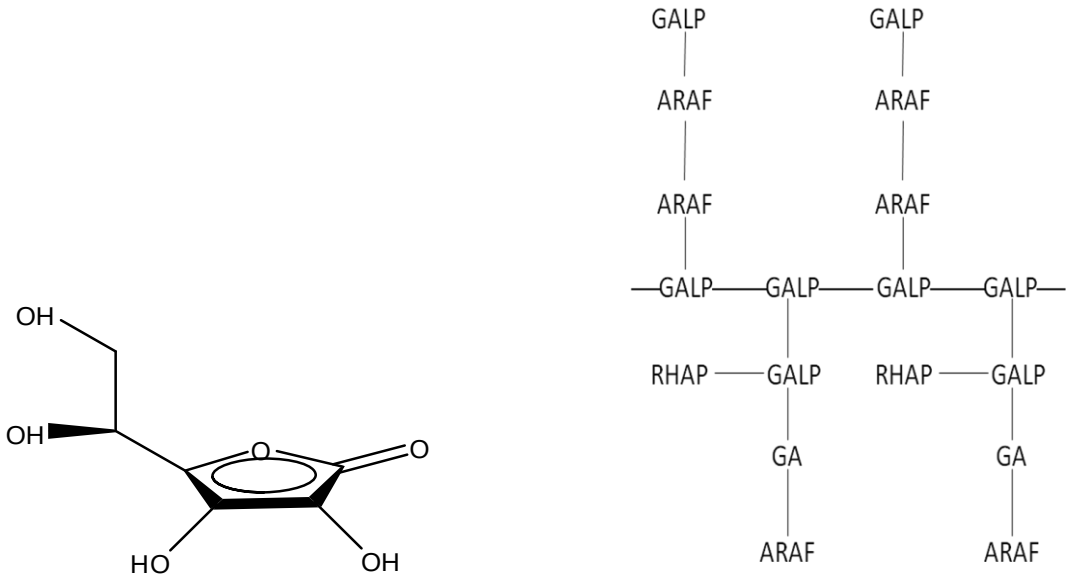

A **B**

Figure 1. Structure of monosaccharides (**A**), Segment of Arabic Gum molecule (**B**). The polysaccharide backbone is composed of D-Galactopyranose (GALP), with linked branches of L-Arabofuranose (ARAF), L-Rhamnopyranose (RHAP), and D-Glucuronic Acid (GA).

Magnetic field usually affects the magnetic species each according to its nature (ferromagnetic, paramagnetic or diamagnetic); one expects that chemical reactions involving such species will be affected if a magnetic field is applied. Moreover, elementary physics shows that charged particles in motion, such as ions, will be subjected to Lorenz force caused by the application of a magnetic field. Lorenz force is proportional to the charge of the ion (q), to its velocity (v) and to the magnetic field (B), taking directions into consideration, through the following equation $\vec{F} = q\vec{v} \times \vec{B}$, and meaning that positive ions and negative ions moving in the same direction will be affected by forces in opposite directions depending on the sign of (q). Moreover, the force should be perpendicular to both *v* and *B*.

Charged chemical species in a solution will have Brownian motion caused by thermal energy. When these particles are subjected to an external magnetic field, their motion will be affected and will be organized accordingly. According to our knowledge, only few studies have been done on the effect of magnetic field on corrosion or generally on chemical reactions [25-30].

The present study seeks to investigate the potential of using *Gum Acacia* as a cheap and environmentally safe corrosion control agent for mild steel in acidic medium with more light on the mechanistic aspects of the corrosion inhibition using potentiodynamic polarization measurement techniques and surface characterization of the formed film due to the interaction between the steel and *Gum Acacia*. Furthermore, contrary to previous studies [27-30], in which the effect of magnetic field on the corrosion of metals was studied under a macroscopic electronic current flow; in this study, the

effect of magnetic field on corrosion was studied in externally applied magnetic fields, in which only permanent magnets were used.

2. EXPERIMENTAL

2.1 Material preparation

Mild steel sheets of composition (0.05% C, 0.32% Mn, 0.027% P, 0.030% S, 0.004% Si and balance Fe) and 0.07 cm thickness were used in the study. The sheets were mechanically press cut into 3×1 cm coupons. These coupons were used as cut with further polishing. However, they were degreased in acetone and rinsed with ether prior to their use in corrosion studies.

2.2 Samples preparation

Gum Acacia (namely, *Gum Arabic* from acacia tree) was obtained from Sigma Chemical (St. Louis, MO). The *Gum Acacia samples* were dissolved in distilled water to prepare solutions of various concentrations ranged from 0.1 to 0.6 mg L^{-1}. The concentrations of hydrochloric acid (HCl) and sulfuric acid (H_2SO_4) prepared and used in the study were 0.5 M, 1.0 M and 2.0 M.

2.3 Weight loss measurements

In the weight loss experiments, the pre-cleaned mild steel coupons were suspended in test tubes containing 15 ml of test solutions maintained at 25°C in a thermo stated bath. The weight loss was determined by retrieving the coupons for 7 days, washed with distilled water cleaned with bristle brush, rinsed with acetone, dried and reweighed. The weight loss was taken to be the difference between the weight at a given time and the original weight of the coupons. The measurements were carried out for the uninhibited solution (blank). Triplicate determinations were carried out. The corrosion rate was computed using the expression:

$$Corrosion rate \quad (CR) = \frac{m_1 - m_2}{At} \tag{1}$$

Where, m_1 and m_2 are the weight loses (mg) before and after immersion in the test solutions, respectively, A is the surface area of the specimens (cm^2) and t is the exposure time (hour).

The inhibition efficiency (I%) of GA was evaluated using the following equation:

$$I\% = \left(\frac{CR_{blank} - CR_{inh}}{CR_{blank}} \right) x100\% \tag{2}$$

Where, CR_{blank} and CR_{inh} are the corrosion rate in the absence and presence of the inhibitor, respectively.

2.4 Hydrogen evolution measurements

The mild steel coupons were pre-cleaned in same way as done in the previous section (weight loss measurement); then it was used for Hydrogen evolution measurements. The test solution was kept at 100 ml. The volume of hydrogen gas evolved when mild steel coupons were dropped into the test solutions was monitored by the depression in the level of paraffin oil. The depression in paraffin oil level was monitored at fixed time interval. The experiment was performed for different concentrations of acidic media (blank), and GA acting as inhibitors in acidic media. The inhibition efficiency (I%) was calculated using the equation:

$$I\% = \left(\frac{V_{blank} - V_{inh}}{V_{blank}} \right) x100\% \quad (3)$$

Where, V_{blank} and V_{inh} are the volume of H_2 gas evolved at time "t" in the absence and presence of the inhibitor, respectively.

For hydrogen evolution method, the rate of dissolution (ml/cm^2.h) was calculated using the following equation:

$$w_{corr} = \frac{V_{H_2}}{St} \quad (4)$$

Where, W_{corr} is the rate of corrosion; V_{H2} is the volume of hydrogen in ml; "S" is the surface area in cm^2 of the metal sheet and "t" is the immersion time per hour.

2.5 Effect of external magnetic field on weight loss and hydrogen evolution measurements

To study the effect of magnetic field on corrosion of mild steel using weight loss and hydrogen evolution methods, the same experimental procedure described in section 2.3 and 2.4 were repeated in externally applied magnetic fields (0.08 T). Prior to each experiment all the solutions were deoxygenated for 15 min by purging with nitrogen gas (Ultra-High purity 99.9995%), using a micro-needle. In the part where magnetic field effect was measured, permanent magnets were used in the experiment by attaching them face to face to the tube in which the sample was located and the magnetic field was measured by inserting a Hall probe (*Leybol-Heraeus*) in the place of the sample and the reading was recorded from a Tesla meter (Gaussmeter H1-R, accuracy ≥2%). Scheme 1 shows the experimental setup for corrosion testing in a magnetic field flux.

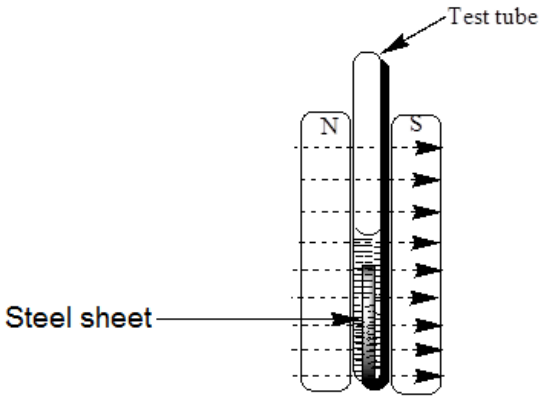

Scheme 1. Experimental setup for studying the magnetic field effect.

2.6 Potentiostatic polarization measurements

Potentiostatic polarization studies were carried out using EG&G (model 264) potentiostat/galvanostat. The current-potential curves were measured using a conventional three-electrode cell. The working electrode was a mild steel sheet (exposed surface area of 0.6 cm^2); saturated calomel electrode (SCE) was used as a reference and a platinum foil was used as counter electrode. Polarization was carried out in hydrochloric acid and sulfuric acid in the absence and presence of various concentrations of the inhibitor (GA). The current-potential curves were recorded automatically. The polarization was scanned from a potential of – 1000 mV to 0.0 mV (SCE) with a scan rate of 10 mV s^{-1}.

The electrochemical corrosion current density was evaluated using the well-known Stern-Geary equation (Eq. 5):

$$I_{corr} = \frac{\beta_a x \beta_c}{2.303(\beta_a + \beta_c)} x \frac{1}{R_p} \quad (5)$$

Where, I_{corr} is the corrosion current density; β_a is the anodic Tafel constant; β_c is the cathodic Tafel constant and R_p is the polarization resistance.

Corrosion current density (*I*corr) was estimated from intercept of cathodic and anodic Tafel lines and the inhibition efficiency (I %) was calculated by using the following equation (Eq. 6)

$$I\% = \frac{I^o_{corr} - I_{corr}}{I^o_{corr}} \quad (6)$$

Where, I_{corr} *and* I^o_{corr} are the corrosion current density with and without the inhibitor, respectively.

2.7 Scanning electron microscopy (SEM)

The surface morphology of the mild steel specimens was examined after polishing and after exposure to 1.0 and 2.0 M hydrochloric acid and sulfuric acid in the absence and presence of optimal concentration of the inhibitor, GA (0.35 mg L^{-1}), using FEI ***Inspect F50*** scanning electronic microscope (Netherlands) equipped with a Field Emission Gun **(*FEG*)**.

2.8 Fourier transform infrared (FTIR) spectroscopy

After the corrosion tests, mild steel specimens subjected to acid solutions in the presence of optimal concentration of the inhibitor, GA (0.35 mg L^{-1}) were thoroughly rinsed with distilled water, dried, and scrapped. The resulting powders were mixed carefully with 6% (w/w) sample/KBr powder ratio and subjected to FTIR analysis. FTIR spectra were recorded with JASCO FTIR-4100 (Japan) spectrophotometer. The FTIR analysis of the Gum Arabic and their iron complex was carried out between 400 and 4000 cm^{-1}.

2.9 X-ray photoelectron spectroscopy (XPS)

The chemical composition of the surface was determined by X-ray photoelectron spectroscopy (XPS) using a UHV apparatus based on a modified Leybold XPS system with a double-anode X-ray source. For the measurements reported here, the Mg K_α phton source (1253.6 eV photons energy) was used. The base pressure of the apparatus was below 3×10^{-10} mbar. High resolution spectra for C1s and O1s lines were recorded with a window of 15 and 20 eV pass energy, corresponding to an experimental resolution of 1.2 eV. All spectra have been deconvoluted with SDP 2.3 XPS-International software, using Gaussian profile lines for peaks fitting.

3. RESULTS AND DISCUSSION

3.1 Weight loss measurements

The effect of addition of *Gum Acacia* on the corrosion of mild steel was studied at different concentration in 0.5 M, 1 M, and 2 M hydrochloric acid and sulfuric acid at 25°C. The results of weight loss of mild steel with time were studied for 7 days (168 h). Table 1 show that the weight loss of mild steel increases as the concentration of acid increases, and the weight loss decrease as the concentration of the inhibitor increases.

The corrosion rates (CR) of mild steel in hydrochloric acid and sulfuric acid decreased with increasing the concentration of *Gum Acacia* until reached the optimal concentration value of 0.35 mg L^{-1} for GA (Fig. 2 and 3). Also Table 1 shows an increase in the corrosion rate with increasing acid concentration. This indicates that the GA in the solution inhibits the corrosion of mild steel in both

acid and the extent of corrosion inhibition depends on the amount of the GA and the acid concentration. Also, the data revealed that GA behaves in hydrochloric acid better than sulfuric acid.

This may be attributed to the fact that chloride ions being less hydrated than sulfate ions and therefore are strongly adsorbed in the metal surface by creating an excess negative charge towards the solution phase, which favors synergistic adsorption in the metal surface. These results are in agreement with several observations of such enhanced efficiency demonstrated by organic inhibitors of mild steel corrosion in hydrochloric acid solutions compared to sulfuric acid *solutions* [31-33]. The optimal concentration obtained in this study was used to further characterize the surface and evaluate the effect of the inhibitor on the corrosion of steel.

Table 1. Weight loss (mg)[a] of mild steel in HCl and H_2SO_4 solutions in the absence and presence of various concentrations of *Gum Acacia* (GA).

[GA] (mg L^{-1})	HCl			H_2SO_4		
	0.5 M	1.0 M	2.0 M	0.5 M	1.0 M	2.0 M
Blank	125.53	338.40	582.80	561.93	909.47	1697.10
0.10	97.20	229.47	358.90	577.23	890.03	1547.90
0.20	97.17	201.03	320.47	518.20	827.17	1604.87
0.30	76.80	166.27	261.60	516.30	803.70	1640.63
0.35	86.43	166.57	264.50	504.47	793.50	1739.17
0.40	77.77	160.70	242.87	504.43	783.33	1614.97
0.45	78.97	130.73	280.13	514.67	587.30	1588.97
0.50	72.40	140.17	267.03	485.13	827.07	1546.47
0.60	69.07	152.50	213.23	499.50	797.23	1462.23

[a]Average triplicate determinations were carried out.

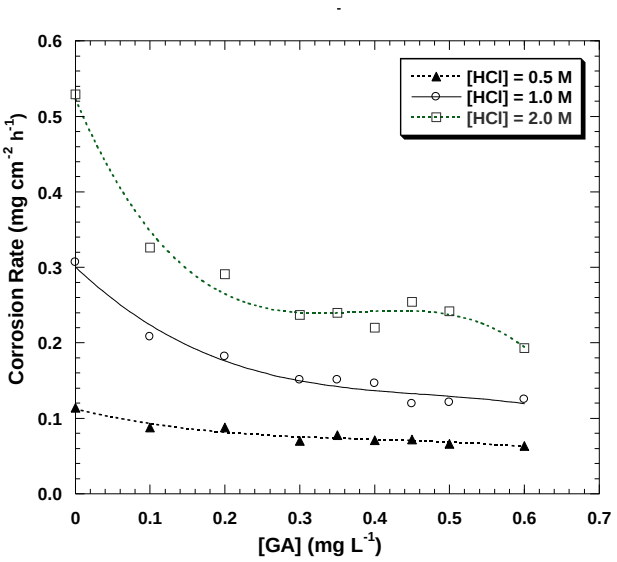

Figure 2. Corrosion rate of steel (mg cm^{-2} h^{-1}) in 0.5, 1.0 and 2.0 M HCl solutions in the absence and presence of various concentrations of *Gum Acacia* (GA) from weight loss measurements. Results are averages of three independent observations.

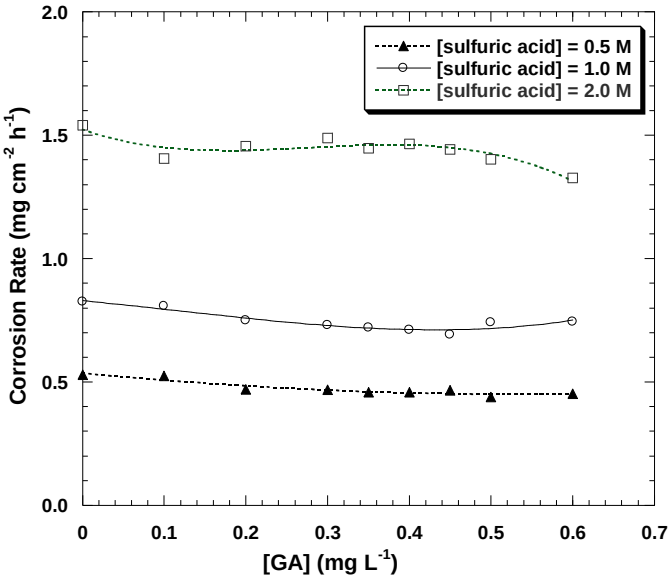

Figure 3. Corrosion rate of steel (mg cm^{-2} h^{-1}) in 0.5, 1.0 and 2.0 M H_2SO_4 solutions in the absence and presence of various concentrations of *Gum Acacia* (GA) from weight loss measurements. Results are averages of three independent observations.

Generally, an increase in inhibition efficiency with the increase in GA concentration due to the adsorption of the GA on the steel metal surface has been observed, the results of the calculated inhibition efficiency of GA for HCl and H_2SO_4 are summarized in Table 2. The adsorption of GA on the mild steel surface makes a barrier for mass and charge transfer. Consequently, the metal is protected from the aggressive anions of the acid. However, the presence of chloride ions from the hydrochloric acid in solution containing GA play a significant role in the adsorption process that results from increased surface coverage as a result of ion-pair interactions between the organic cations and the chloride ions.

Table 2. Inhibition efficiency (I%) of GA for HCl and H_2SO_4 from weight loss measurement.

[GA] (mg L^{-1})	HCl			H_2SO_4		
	0.5 M	1.0 M	2.0 M	0.5 M	1.0 M	2.0 M
Blank	---	---	---	---	---	---
0.10	22.81	32.25	38.37	01.13	02.18	08.77
0.20	22.81	40.72	44.99	11.32	09.09	05.45
0.30	38.60	50.81	55.20	11.70	11.13	03.31
0.35	31.58	50.81	54.63	13.58	12.73	05.97
0.40	37.72	52.44	58.41	13.58	13.82	04.87
0.45	36.84	61.24	51.98	11.89	16.12	06.36
0.50	42.11	60.59	54.25	16.98	10.06	08.90
0.60	44.74	59.28	63.52	14.53	09.82	13.83

This observation is in agreement with earlier published reports [31-33]. Another possibility may be due to the formation of positively charged protonated GA (since it contains glucoproteins) species in acidic solution, which facilitates adsorption on the metal surface through a coordinate type of linkage. The degree of protection increases with increase in GA concentration due to higher degree of surface coverage resulting from enhanced inhibitor adsorption

Further investigation using surface analytical techniques below enabled the characterization of the active materials in the adsorbed layer and assist in identifying the most active ingredients.

3.2 Hydrogen evolution measurements

The effect of addition of *Gum Acacia* on the corrosion of mild steel was studied at different concentration in 0.5 M, 1 M, and 2 M hydrochloric acid and sulfuric acid at 25°C. The results of hydrogen evolution of mild steel with time were studied for 7 days. Similar to what have been observed for weight loss measurements, the hydrogen evolution of mild steel increases as the concentration of acid increases, and the hydrogen evolution decrease as the concentration of the inhibitor increases. The corrosion rate increased with increasing acid concentration, and an increase in inhibition efficiency with the increase in GA concentration due to the adsorption of the GA on the steel metal surface has been observed, the results of the calculated corrosion rate and inhibition efficiency of GA for HCl and H_2SO_4 are summarized in Tables 3 and 4, respectively. This indicates that the GA in the solution inhibits the corrosion of mild steel in acidic media and the extent of corrosion inhibition depends on the amount of the GA and the acid concentration.

Table 3. Corrosion rate[a] ((ml cm^{-2} h^{-1}) of mild steel in HCl and H_2SO_4 solutions in the absence and presence of various concentrations of *Gum Acacia* (GA) from Hydrogen evolution measurements.

[GA] (mg L^{-1})	HCl			H_2SO_4		
	0.5 M	1.0 M	2.0 M	0.5 M	1.0 M	2.0 M
Blank	7.20	8.50	10.20	8.50	10.40	12.30
0.10	5.35	5.78	6.00	8.30	10.10	11.70
0.20	5.14	5.00	5.50	7.40	9.35	11.60
0.30	4.35	4.40	4.70	7.30	9.20	11.55
0.35	4.20	4.05	4.51	7.20	9.00	11.50
0.40	4.07	3.85	4.15	7.10	8.90	11.45
0.45	3.78	3.20	3.85	7.01	8.70	11.30
0.50	3.50	3.11	3.50	6.90	8.60	11.10
0.60	3.29	2.98	3.41	6.85	8.50	10.50

[a]Average triplicate determinations were carried out

Table 4. Inhibition efficiency (I%) of GA for HCl and H_2SO_4 from Hydrogen evolution measurements.

[GA] (mg L^{-1})	HCl			H_2SO_4		
	0.5 M	1.0 M	2.0 M	0.5 M	1.0 M	2.0 M
Blank	---	---	---	---	---	---
0.10	25.70	32.00	41.18	02.35	02.88	04.88
0.20	28.61	41.17	46.08	12.94	10.10	05.70
0.30	39.58	48.23	53.92	14.12	11.54	06.10
0.35	41.67	52.35	55.78	15.29	13.46	06.50
0.40	43.47	54.70	59.31	16.47	14.42	06.90
0.45	47.50	62.35	62.25	17.52	16.35	08.13
0.50	51.40	63.41	65.68	18.80	17.31	09.76
0.60	54.30	64.94	66.56	19.41	18.27	14.63

3.3 Effect of magnetic field

The weight loss and Hydrogen evolution measurements for *Arabic Gum* show the same trend in the presence and absence of an external applied magnetic field, with remarkable reduction in the weight loss in the presence of magnetic field (Tables 5 and 6). The obtained results reveal that the weight loss of steel in the presence of magnetic field was less than that in the absence of magnetic field at the same range of concentrations of inhibitor. Thus, an applied magnetic field enhances the rate of passivation (formation of passive layer) on the surface [34].

The formation of passive layer increased as the inhibitor concentration increases. Therefore, the inhibition of the corrosion of steel with addition of the inhibitor was enhanced in the presence of magnetic field because passivation was enhanced. The magnetic field effects may be explained by the Lorentz force [26]. The magnetic field will make the *Arabic Gum* molecules to align on the surface of the metal rather than randomly laying down on the surface.

Table 5. Inhibition efficiency (I%) of GA for HCl and H_2SO_4 by weight loss method, in an externally applied magnetic field (0.08 T), at room temperature. Immersion time 7 days.

[GA] (mg L^{-1})	HCl			H_2SO_4		
	0.5 M	1.0 M	2.0 M	0.5 M	1.0 M	2.0 M
Blank	---	---	---	---	---	---
0.10	32.70	37.10	41.56	05.61	06.10	10.50
0.20	34.50	42.65	45.78	15.50	16.00	11.45
0.30	39.70	48.90	55.05	18.90	19.13	12.40
0.35	44.75	54.80	59.60	22.50	23.70	13.90
0.40	48.60	57.57	62.70	24.55	25.02	14.80
0.45	52.75	63.54	65.00	27.90	27.00	15.25
0.50	55.55	67.90	69.15	30.00	30.50	15.95
0.60	59.80	72.80	75.60	34.50	35.00	16.80

Table 6. Inhibition efficiency (I%) of GA for HCl and H_2SO_4 by Hydrogen evolution method, in an externally applied magnetic field (0.08 T), at room temperature. Immersion time 7 days.

[GA] (mg L^{-1})	HCl			H_2SO_4		
	0.5 M	1.0 M	2.0 M	0.5 M	1.0 M	2.0 M
Blank	---	---	---	---	---	---
0.10	35.00	39.10	43.90	06.50	07.80	10.80
0.20	38.50	43.56	48.34	17.90	18.15	11.70
0.30	40.90	50.50	56.90	19.50	20.54	12.18
0.35	45.65	55.65	60.80	23.19	25.90	13.58
0.40	49.78	59.10	63.70	25.48	26.92	14.95
0.45	53.50	65.15	67.15	29.02	30.65	15.33
0.50	56.40	69.26	70.87	31.10	32.11	16.78
0.60	60.20	75.90	77.80	36.80	37.29	17.80

Based on the results that were summarized in Tables 5 and 6, one can conclude that the presence of inhibitor and external magnetic field is needed to reach high inhibition of corrosion of steel in acidic solutions, but more recognized in HCl than in H_2SO_4.

The results obtained reveal that the weight loss of steel in the presence of a magnetic field was less than that in the absence of a magnetic field at the same concentration range of the inhibitor. Thus, an applied magnetic field appeared to assist the rate of passivation (formation of iron oxide) on the surface. The formation of iron oxide film increased with increasing the inhibitor concentration. Therefore, the inhibition of the corrosion of steel with addition of the inhibitor was enhanced in the presence of magnetic field because passivation was enhanced. Moreover, apart from the option of enhanced passivity it seems that the *Arabic Gum* and the magnetic fields could have also affected wetting of the steel surface and the concentration gradients of the ionic species in this chemically active surface boundary layer.

According to our results, we suggest that the magnetic field could affect the structure of the repassivating deposits of *Arabic Gum*. We came to the conclusion that under the influence of magnetic field the initial *Arabic Gum* molecules reoriented themselves in such a way that the interaction energy between the *Arabic Gum* molecules and magnetic field would become minimal. In Addition, the observed corrosion magneto inhibition effect could be explained in terms of field assisted formation of the oxides with higher degree of dispersion. This effect was evident from the decrease in mass loss.

3.4 FTIR

The FTIR spectrum of GA-steel complexes is obtained by rubbing KBr powder on steel sheets after immersing them in acidic media (hydrochloric acid and sulfuric acid) with 0.35 mg/L of GA for 7 days. Also, the FTIR spectrum of GA powder is obtained between 400 and 4000 cm^{-1}.

Fig. 4 shows the FTIR spectra of GA and GA-steel complex in various concentrations of hydrochloric acid (4-A) and sulfuric acid (4-B). As can be seen from the FTIR shown in Fig. 4, the spectrum exhibits very clear and strong features assigned to the polysaccharide molecules in GA. The

major and strongest vibrational modes in the GA spectrum are these located at 1068, 1429, 1626, 2365, 2924, and a broad absorption band at 3000-3600 cm^{-1}. In addition to these major peaks, an additional peak appears at low frequency with low intensity at 650 cm^{-1}. The strong vibrational mode located at 3000-3600 cm^{-1} is assigned to the stretching vibrations of the O–H bond, the other strong vibrational mode located at 1626 cm^{-1} is assigned to the stretching vibrations of the C=O bond of carboxylate group associated with the GA molecules, the two vibrational modes located at 1068 and 1429 cm^{-1}, with relatively low intensity, are assigned to the stretching vibrations of the C–O bond, and the weak vibrational mode located at 2924 cm^{-1} is assigned to the stretching vibrations of the C–H bond [35]. The absorption band located at 2365 cm^{-1}, with relatively low intensity, is usually assigned to the CO_2 vibration [35]. It is worth mentioning that GA is made up of large amount of polysaccharide and very less amount of glycoprotein [35]. However, according to the FTIR spectra shown in Figure 3, no significant absorption bands have been observed for glycoprotein molecules. This result is attributed to the presence of broad absorption band at 3000–3600 cm^{-1} due to the O–H stretch of polysaccharide which might cover the characteristic bands of glycoprotein molecules.

In order to address the adsorption of GA onto the surface of steel and the possible formation of GA-steel complex, it is most instructive to compare the relative intensities of the major vibrational modes of plain GA spectrum to those of the of GA-steel complexes spectrum that is obtained by rubbing KBr powder on steel sheets after immersing them in acidic media. Close inspection of Fig. 4 (A and B), which shows the FTIR spectra of GA and GA-steel complex in 0.5 and 1.0 M aqueous solutions of hydrochloric acid (A) and sulfuric acid (B), reveals the presence of very interesting features. The weak vibrational mode located at 2924 cm^{-1}(C–H stretch) is vanished completely in the GA-steel complex spectra in acidic media. The major bands concerning the stretching vibrations of the O–H bond at 3000-3600 cm^{-1} and the stretching vibrations of the C=O bond of carboxylate group associated with the GA molecule at 1626 cm^{-1}, for which a decrease in intensity is observed in the GA-steel complex spectra in both acidic media. The two vibrational modes concerning the stretching vibrations of the C–O bond located at 1068 and 1429 cm^{-1}, for which a decrease in intensity and shift to lower wave numbers is observed in the GA-steel complex spectra in both acidic media. Furthermore, a large reduction of the relative intensities of all major bands as we go from high to lower concentration of acid is observed. Interestingly, the reduction of the intensities of all major bands in hydrochloric acid is much more than those in sulphuric acid due to the synergistic effect of chloride ions on the corrosion inhibition of mild steel. Moreover, the shift to lower wave numbers that were observed for the stretching vibrations of the C–O bond located at 1068 and 1429 cm^{-1} in the GA-steel complex spectra in hydrochloric acid is much more than those in sulphuric acid and the bands are more broaden in sulphuric acid; such behaviour can be attributed to the presence of adsorbed and free polysaccharide molecules on the surface of steel in sulphuric acid medium while in hydrochloric acid medium most of the polysaccharide molecules are adsorbed on the surface of the steel.

The overall features of the FIIR spectra shown in Fig. 4 suggested that there is a strong adsorption of GA onto the surface of the steel, which is more pronounced in hydrochloric acid than sulphuric acid, due to the electrostatic binding of the carboxylate groups of the GA molecule to sites along oxide surfaces of steel [36]. This conclusion was interpreted from the large reduction of the intensities of all prominent bands and the shift in position of the stretching vibrations bands of the C–O

bond in GA-steel complex spectra relative to plain GA spectrum. Our findings are very well in agreement with the previous results obtained for adsorption of GA on magnetic nano-particles [35,36].

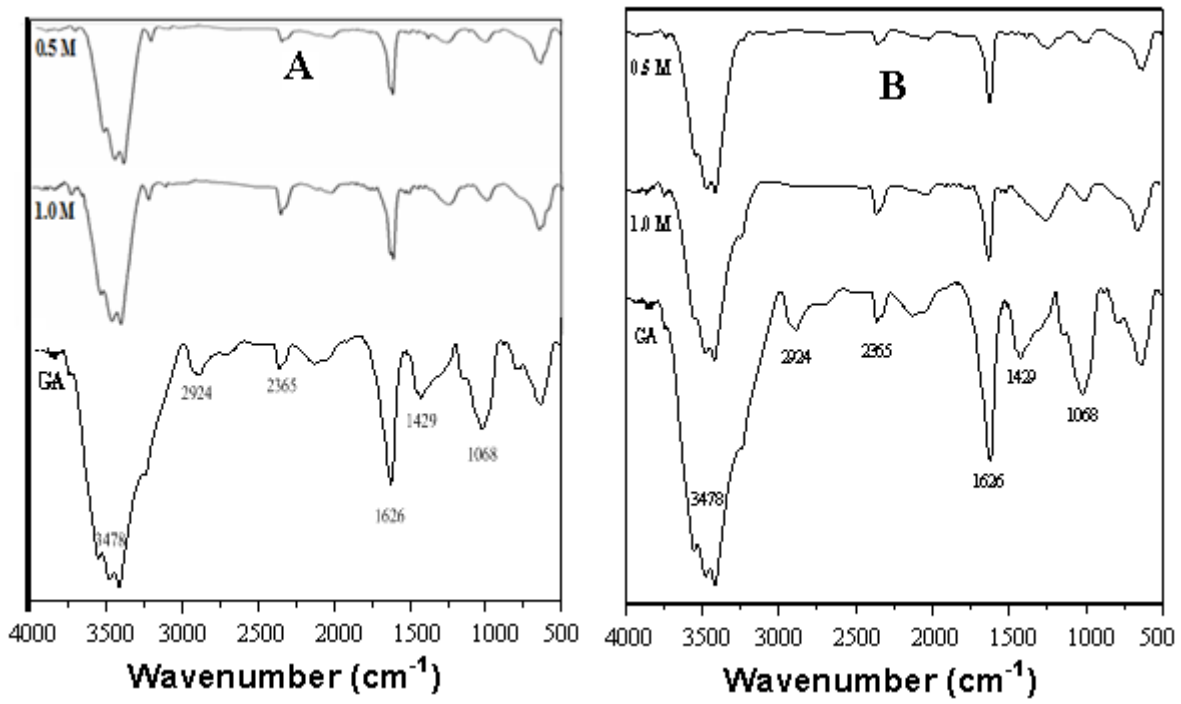

Figure 4. FTIR spectra for *Gum Acacia* (GA) and GA-steel complex in **(A)** 0.5 and 1.0 M HCl, and **(B)** 0.5 and 1.0 M H_2SO_4 solution.

3.5 Scanning electron microscope (SEM)

The surface morphology of treated mild steel assessed by scanning electron micro- scope is shown in Fig. 5 for samples treated with 1.0 M hydrochloric acid solution and Fig. 6 for samples treated with 1.0 M sulfuric acid solution. Each figure shows scanning electron micrographs of the tested surfaces with and without inhibitor. Furthermore, both figures show the surface morphology of plain mild steel. Scanning electron micrograph of plain mild steel shows parallel grooves with relatively light areas, which were identified as clean surface. Fig. 5 shows the surface morphology of plain mild steel and mild steel exposed to 1.0 M hydrochloric acid in the presence and absence of 0.35 mg L^{-1} GA. Fig. 6 shows the surface morphology of plain mild steel and mild steel exposed to 1.0 M H_2SO_4 in the presence and absence of 0.35 mg L^{-1} GA. A uniform severe corrosion can be observed in the absence of inhibitor for the two acids (Fig. 5 and 6), showing adherent amorphous corrosion products.

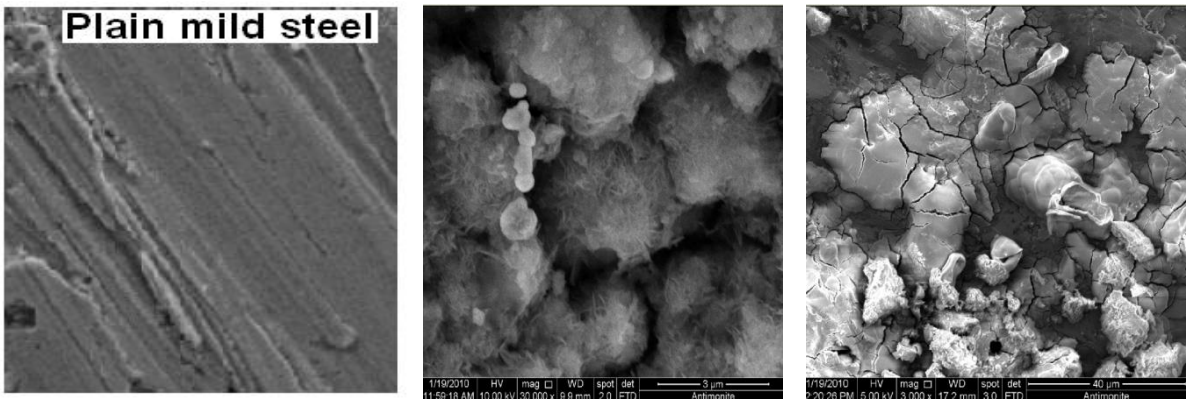

(A) Mild Steel (B) without inhibitor (C) with inhibitor

Figure 5. Scanning electron micrograph of plain mild steel **(A)** mild steel in 1.0 M HCl, **(B)** mild steel in 1.0 M HCl without inhibitor and **(C)** mild steel in 1.0 M HCl in the presence of 0.35 mg/l GA at 25 °C.

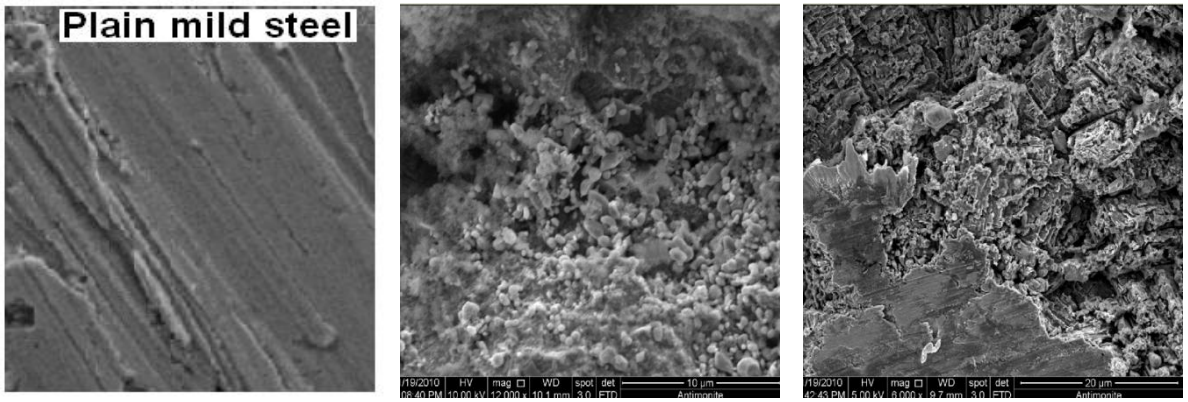

(A) Mild Steel (B) without inhibitor (C) with inhibitor

Figure 6. Scanning electron micrograph of plain mild steel **(A)** mild steel in 1.0 M H_2SO_4, **(B)** mild steel in 1.0 M H_2SO_4 without inhibitor and **(C)** mild steel in 1.0 M H_2SO_4 in the presence of 0.35 mg L^{-1} GA at 25 °C.

However, the SEM obtained for mild steel in presence of inhibitor showed that the metal surface is partially covered with inhibitor giving it a reasonable degree of protection and it is obvious that the surface is more covered with inhibitor in presence of hydrochloric acid (Fig. 5) than sulfuric acid (Fig. 6). The formation of an adsorbed protective film of the inhibitor molecules on the mild steel surface is also confirmed by scanning electron micrographs in Fig. 5 and 6, which proves that the *Gum Acacia* acts as good inhibitor at 1.0 M acids concentration.

Scanning electron micrographs of the tested surfaces in 1.0 M HCl and presence of 0.35 mg/L GA at 25°C with applied magnetic field are shown in Figure 7. Fig. 7 shows the photomicrographs with different magnification of a sheet surface in the presence of magnetic field (0.08 T). Scanning electron micrograph (view 1 Fig. 7), show parallel grooves with relatively light and dark (hole) areas, which were identified as clean (A) and corroded regions (B). The light area was identified as location

B, and the dark (hole) area was identified as location A. Higher magnification views at locations A and B are shown in views 2 and 3 Fig. 7, respectively, in which a parallel grooves are evident in these areas. Higher magnifications view at the center of view 3 Fig. 7 show adherent amorphous deposits (view 4 Fig. 7). The photomicrographs in views 1-4, Fig. 7, show the preferential increase in the formation of iron oxide, which could be due to the application of the magnetic field on the steel sheet.

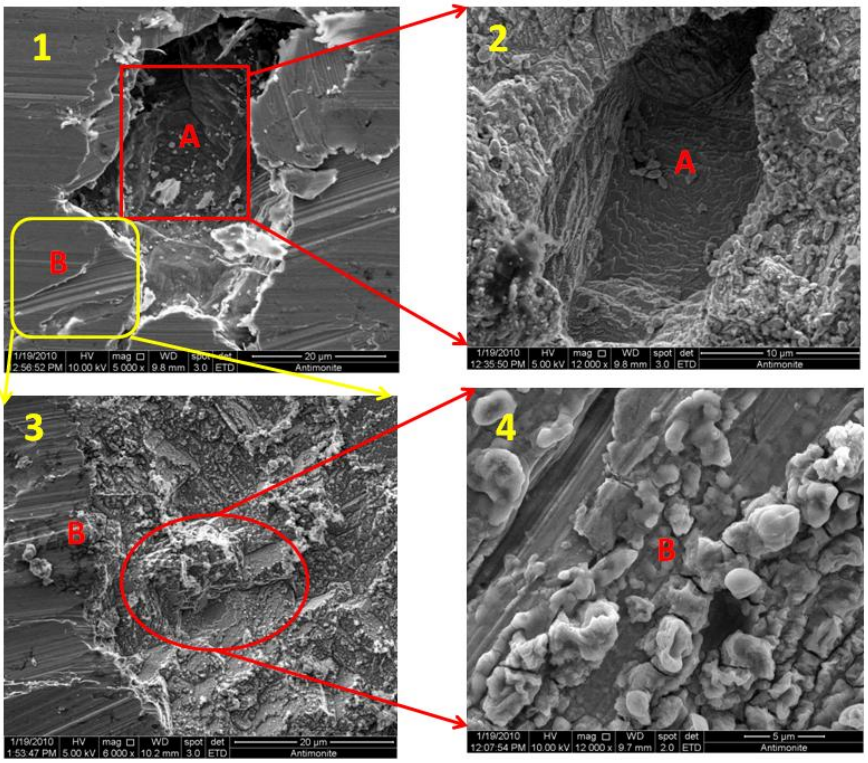

Figure 7. Scanning electron micrographs of the mild steel surfaces (views 1-4) in the presence of applied magnetic field (0.08 T). Immersion time 2 h, in 1.0 M HCl and presence of 0.35 mg/l GA at 25°C.

3.6 XPS Analysis

The XPS results were performed to identify the characteristic elements for the system of mild steel and inhibitor ([GA] = 0.35 mg L^{-1}) in the aqueous solution of 1.0 M HCl. The extended spectrum shows two major elements on the surface, at binding energy 285.2 and 532 eV corresponding to C 1s and O 1s, respectively. The XPS peaks of other elements, which are mainly from the mild steel substrate chemical composition) are observed with small intensities, this indicates that the substrate is almost completely covered by the inhibitor. Fig. 8 A and B depicts the high resolution XPS spectra for the C 1s and O 1s regions, respectively. These peaks were assigned to the corresponding species through a deconvolution fitting procedure; the peak identification of characteristic elements was in agreement with suitable databases [37,38]. The binding energies at 287 eV for C 1s and 532.95 eV for

O 1s confirm the binding of the inhibitor (GA) on the surface of steel. Other peaks in Fig. 8 confirm that GA forms a stable and uniform layer grown from the solution on the mild steel surface.

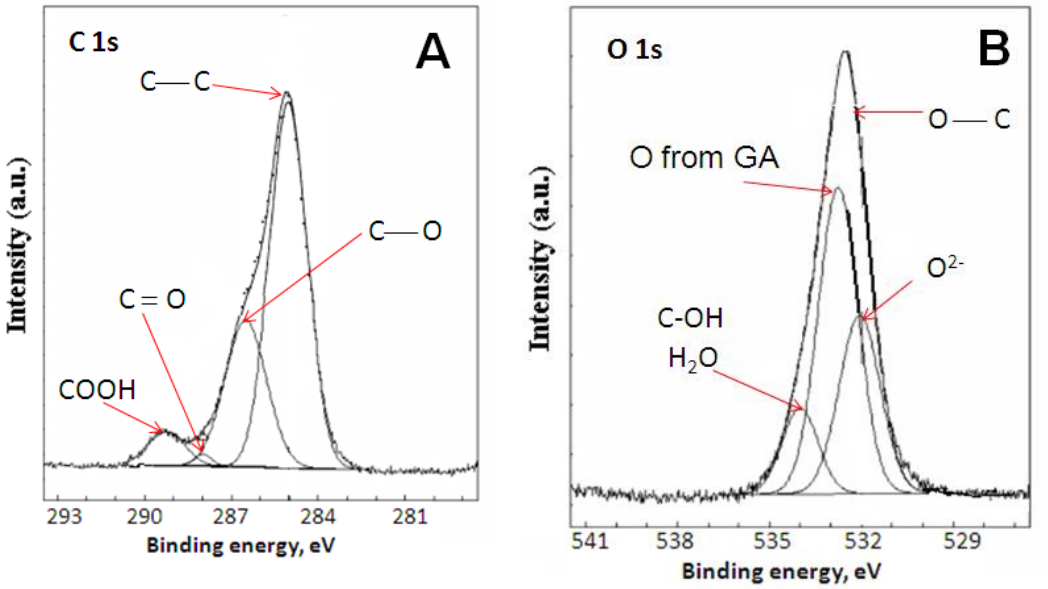

Figure 8. XPS spectra for C 1s (**A**) and O 1s (**B**) regions of mild steel in presence of 0.35 mg L^{-1} of inhibitor (GA) in 1.0 M HCl, at room temperature.

The C 1s spectrum (Fig. 8A) shows four-peak profile indicative of four chemical forms of C present on the steel surface. The largest peak was assigned to the C-C aliphatic bonds with a characteristics binding energy of 285.2 eV, whereas the other three may be assigned to the C-O (286.75 eV), C=O (288 eV) and COOH (289.4 eV) bonds. The concentration of C on the steel surface was approximately determined to be 65 atomic percent; this content can only be related to the carbon rich structure of the GA. The presence of Oxygen on the steel surface indicated that the surface becomes oxidized, which is a typical effect of the test solution. Similar to C 1s, the O 1s spectrum shows four-peak profile indicative of four chemical forms of O present on the steel surface (Fig. 8B). The largest peak was assigned to the C-O bonds with a characteristics binding energy of 532.8 eV, whereas the other three may be assigned to the O from GA (533 eV), C-OH and H_2O (534.1 eV) and the most important peak at 532.2 eV assigned to O^{2-} molecules; this confirms the interaction between GA and the oxide layer on the steel surface.

3.7 Potentiostatic polarization measurements

The polarized anodic and cathodic potentials were reported in the absence and presence of various concentration of GA (inhibitor) in a current density range of 1.25-5.0 μA cm^{-2} for sulfuric acid and 0.25-4.5 μA cm^{-2} for hydrochloric acid. Fig. 9 and 10 show the cathodic and anodic polarization

curves of mild steel in the absence and presence of various concentrations of inhibitor in 1.0 M of sulfuric acid and hydrochloric acid, respectively.

The electrochemical corrosion parameters including corrosion potential (E_{corr}), corrosion current density (I_{corr}), anodic Tafel constant (β_a), cathodic Tafel constant (β_c) and inhibition efficiency ($I\%$) were calculated from the polarization curves of mild steel in the absence and presence of various concentrations of inhibitor in 1.0 M of sulfuric acid and hydrochloric acid and summarized in Tables 7 and 8, respectively. The electrochemical corrosion parameters summarized in Tables 7 and 8 show that the corrosion current density is markedly reduced as the concentration of inhibitor increases, which indicates that the GA has a pronounced corrosion inhibition effect of mild steel in acidic media. From the shape of the polarization curves (Fig. 9 and 10) it is obvious that both anodic and cathodic reactions are inhibited. It is evident from the data shown in Tables 7 and 8 that as the concentration of the inhibitor increases, the corrosion potential (E_{corr}) is not changing significantly and lower corrosion current density (I_{corr}) values are obtained. Moreover, the values of both anodic (β_a) and cathodic (β_c) Tafel constants are strongly changed in the presences of the inhibitor.

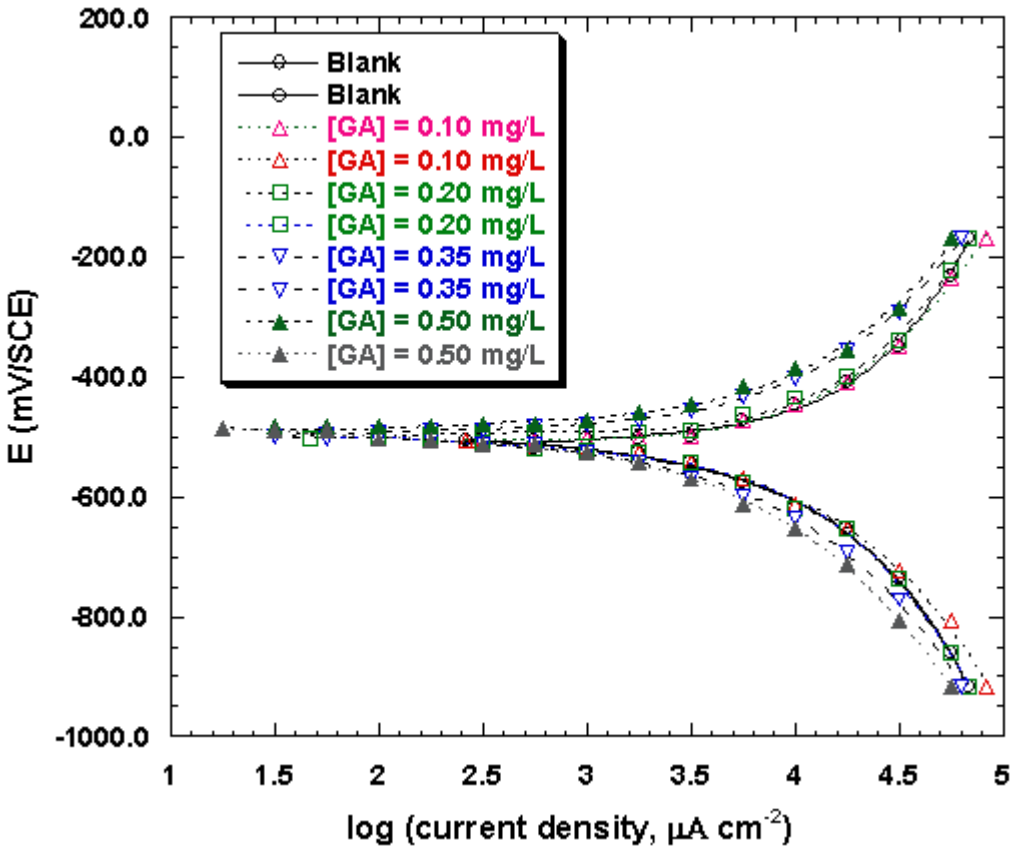

Figure 9. Polarization anodic and cathodic curves of mild steel in the absence and presence of various concentrations of GA in 1.0 M H_2SO_4.

This confirms the mixed mode (anodic and cathodic) inhibition action of the *Gum Acacia*. As shown in Tables 7 and 8, it is obvious that the anodic Tafel constant (β_a) is greater than the cathodic

(β_c) Tafel constant at all inhibitors' concentrations suggesting that the inhibitors' effect on the anodic polarization is more pronounced than that on cathodic polarization. Furthermore, inspection of Tables 7 and 8 reveals that the inhibition efficiency (I%) increases with increasing the concentration of inhibitor. The obtained values of inhibition efficiency (I%) from polarization study were in good agreement with those obtained from the weight loss study with small variation.

The polarization anodic and cathodic curves of mild steel in the absence and presence of various concentrations of GA in 1.0 M H_2SO_4 (Fig. 9) showed similar behavior as those in 1.0 M hydrochloric acid (Fig. 10), but the calculated inhibition efficiency (I%) in sulfuric acid is much less than those in hydrochloric acid.

Table 7. Electrochemical corrosion parameters of mild steel in the absence and presence of various concentrations of inhibitor (GA) in 1.0 M H_2SO_4.

[Inhibitor] (mg L^{-1})	E_{corr} (mV/SCE)	I_{corr} (μA cm^{-2})	β_a (mV/decade)	β_c (mV/decade)	I%
Blank	-506.6	2981.12	195.34	127.56	-
0.10	-505.2	2890.50	132.56	103.76	3.04
0.20	-501.5	2702.45	112.34	93.12	9.35
0.35	-497.3	2670.56	140.51	96.35	10.42
0.50	-486.1	2600.67	81.78	63.69	12.76

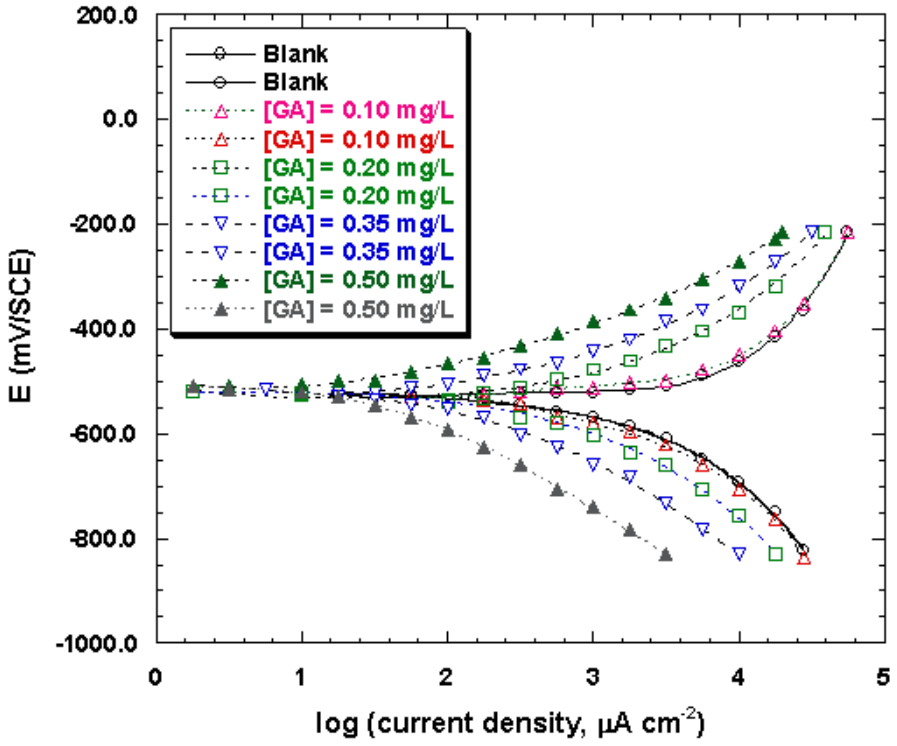

Figure 10. Polarization anodic and cathodic curves of mild steel in the absence and presence of various concentrations of GA in 1.0 M HCl.

Table 8. Electrochemical corrosion parameters of mild steel in the absence and presence of various concentrations of inhibitor (GA) in 1.0 M HCl.

[Inhibitor] (mg L^{-1})	E_{corr} (mV/SCE)	I_{corr} (μA cm^{-2})	β_a (mV/decade)	β_c (mV/decade)	I%
Blank	-528.8	5235.56	210.45	148.67	-
0.10	-525.4	3500.45	140.78	108.56	33.14
0.20	-519.6	3005.78	130.67	99.89	42.59
0.35	-516.8	2520.78	134.09	89.45	51.85
0.50	-508.5	1998.50	145.05	79.89	61.82

The results of both weight loss and polarization methods revealed that the *Gum Acacia* provide a very good protection to mild steel against corrosion in hydrochloric acid medium more than that in sulfuric acid. This can be attributed to the relative stability of the *Gum Acacia* film that formed on the surface of mild steel due the synergistic effect as a result of ion pair interactions between the *Gum Acacia* and the chloride ions.

4. CONCLUSIONS

The following points can be concluded from this research:

1. The results from weight loss, hydrogen evolution, and polarization methods proposed the potential applicability of *Gum Acacia* as a green corrosion inhibitor for mild steel in acidic media.

2. The protection efficiency in HCl is much more than that in sulfuric acid due to the synergistic effect of chloride ions on the corrosion inhibition of mild steel.

3. Polarization measurements showed that the inhibitor (GA) is a mixed type inhibitor (anodic and cathodic).

4. The FTIR results showed that there is a strong adsorption of GA on the surface of the steel via the formation of GA-steel complex. This complex is formed on the steel surface with mono- or bidentate bonds between the carboxylate and steel surface.

5. The SEM results showed that the metal surface is partially covered with the inhibitor giving it a reasonable degree of protection and the surface is more covered with inhibitor in HCl than H_2SO_4. These results are in agreements with the FTIR results.

6. Results are consistent with those obtained by FTIR, XPS, and SEM analysis, which suggested that the protection mechanism was due to the adsorption of GA on the steel surface which enhanced the steel properties against corrosion.

7. In addition, there is quite an increase in the inhibition efficiency (I%) in the presence of magnetic field. Thus, the presence of a magnetic field suppresses corrosion reactions of mild steel with addition of the inhibitor (GA) in acidic media at room temperature. In the absence of GA, the corrosion reactions increase with increasing magnetic flux density as a result of the higher dissolution of steel.

8. The *Arabic Gum* is a beneficial inhibitor for steel corrosion in acidic medium in the presence

and absence of external magnetic field. Its ability as an inhibitor differs in the presence and absence of external magnetic field. This is probably due to the differences of mode of adsorption, and perhaps the field-assisted formation of the oxide layer with a superior capacity to pit re-passivation.

ACKNOWLEDGEMENTS
The author M.A. Abu-Dalo acknowledges the financial support of the Jordan University of Science and Technology Research Fund. N.A.F. Al-Rawashdeh acknowledges the financial support of the UAEU (Project No.: 31S014).

References

1. A.F. Fouda, H.A. Mostafa, S.E. Ghazy and S.A. El-Farah, *Int. J. Electrochem. Sci*. 2 (2007) 182-194.
2. A.K. Maayta and N.A. Al-Rawashdeh, *Corros. Sci.* 46(5) (2004) 1129–1140.
3. N.A.F. Al-Rawashdeh, A.K. Maayta, *Anti-Corros. Methods Mater*. 52(3) (2005) 160-166.
4. M.D. Shah, V.A. Panchal, G.V. Mudaliar and N.K. Shah, *Anti-Corros. Methods Mater.*, 58(3) (2011) 125-130.
5. S.S. Abd El Rehim, M.A.M. Ibrahim and K.F. Khaled, *Mater. Chem. Phys.* 70(3) (2001) 268–276.
6. I. Dehri and M. Ozcan, *Mater. Chem. Phys.* 98(3) (2006) 316–323.
7. H.S. Shukla, N. Haldar and G. Udaybhanu, *J. Corros. Sci. Eng*. 14(28) (2011) 1-18.
8. G. Gunasekaran and L.R. Chauhan, *Electrochimica Acta* 49(25) (2004) 4387-4395.
9. S. Rekkab, H. Zarrok, R. Salgi, A. Zarrouk, Lh. Azzi, B. Hammouti, Z. Kabouche, R. Touzani and M. Zougagh, *J. Mat. Environ. Sci.* 4 (2012) 613-627.
10. A. Ostovari, S.M. Hoseinieh, M. Peikari, S.R. Shadizadeh and S.J. Hashemi, *Corros. Sci.* 51(9) (2009) 1935-1949.
11. R.P. Bothi, R.A. Abdul, O. Hasnah and A. Khalijah, *Acta. Phys. Chim. Sin.* 26(8) (2010) 2171-2176.
12. P.B. Raja and M.G. Sethuraman, *Mater. Corr.* 60 (1) (2009) 22-28.
13. O.K. Abiol and A.O. James, *Corros. Sci.* 51(8) (2009) 1879-1881.
14. M. Sangeetha, S. Rajendran, T.S. Muthumegala and A. Krishnaveni, *Zaštite Materijala* 52(1) (2011) 3-19.
15. H.A. Swenson, H.M. Kaustinen, O.A. Kaustinen and N.S. Thompson, *J. Polym. Sci. Part-A-2* 6 (1968) 1593-1606.
16. Y. Dror, Y. Cohen and R. Yerushalmi-Rozen, *J. Polym. Sci.* 44 (2006) 3265-3271.
17. D. Verbeken, S. Dierckx and K. Dewettinck, *Appl. Microbiol. Biotechnol.* 63(1) (2003) 10–21.
18. O.H.M. Idris, P.A. Williams and G.O. Phillips, *Food Hydrocoll.* 12(4) (1998) 379–388.
19. M.A. Yadav, J.M. Igartuburu, Y. Yan and E.A. Nothnagel, *Food Hydrocoll.* 21 (2007) 297–308.
20. K.A. Karamalla, N.E. Siddig and M.E. Osman, *Food Hydrocoll*. 12(4) (1998) 373-378.
21. S.A. Umoren, I.B. Obot, E.E. Ebenso and N.O. Obi-Egbedi, *Int. J. Elecrochem. Sci.* 3(9) (2008)1029-1043
22. S.A. Umoren, I.B. Obot, E.E. Ebenso, N.O. Obi-Egbedi and R. Hookeri, *Desalination* 247(3) (2009) 561-572.
23. S.A. Umoren, I.B. Obot, E.E. Ebenso, P.C. Okafor, O. Ogbobe and E.E. Oguzie, *Anti-Corrosion Methods and Materials* 53(5) (2006) 277- 282.
24. S.A. Umoren, *Cellulose* 15(5) (2008) 751-761.
25. A.K. Maayta and N.A.F. Al-Rawashdeh, *Jordan J. Chem.* 5(2) (2010) 175-189.
26. A. Ruosan and N.A.F. Al-Rawashdeh, *Corros. Eng. Sci. Tech.* 41(3) (2006) 235-239.
27. K. Shinohara and R. Aogaki, *Electrochem.* 67 (1999) 126.

28. A. Chiba, K. Kawazu, O. Nakano, T. Tamura, S. Yoshihara and E. Sato, *Corros. Sci.* 36 (1994) 539.
29. A. Rucinskiene, G. Bikulcius, L. Gudaviciute and E. Juzeliunas, *Electrochem. Comm.* 4 (2002) 86.
30. Y.P. Ma, J.P. Wikswo, M. Samuleviciene, K. Leinartas and E. Juzeliunas, *J. phys. Chem. B.* 106 (2002) 12549.
31. E.A. Noor, *Int. J. Electrochem. Sci.* 2(12) (2007) 996 – 1017.
32. M.A. Quraishi and D. Jamal, *Mater. Chem. Phys. 78(3)* (2003) *608*–613.
33. T.Y. Soror *and* M.A. El-Ziady, *Mater. Chem. Phys. 77(3) (*2002) *697*-703.
34. A. Chiba, K. Kawazu, O. Nakano, T. Tamura, S. Yoshihara and E. Sato, *Corros. Sci.* 36 (1994) 539-543.
35. S.S. Banerjee and D-H. Chen, *J. Hazardous Material* 147(3) (2007) 792-799.
36. D. N. Williams, K. A. Gold, T. R. Pulliam Holoman, S. H. Ehrman and O. C. Wilson Jr., *J. Nanoparticle Research* 8(5) (2006) 749-753.
37. D. Briggs and M.P. Seah (Eds.), *Practical surface analysis, 2nd Ed., Auger and X-Ray Photoelectron Spectroscopy*, Vol. 1, John Wiley & Sons, Chichester, England, (1990).
38. F. Moulder, W.F. Stickle, P.E. Sobol and K.D. Bomben, in J. Chastain (Ed.), *Handbook of X-Ray Photoelectron Spectroscopy*, Perkin-Elmer Copr., Minnesota, USA (1992).